Data in Brief 55 (2024) 110565

Contents lists available at ScienceDirect

Data in Brief

journal homepage: www.elsevier.com/locate/dib

Data Article

Insilico evaluation on potential *Mt-Sp1/matriptase* inhibitors data: DFT and molecular modelling approaches

Abel Kolawole Oyebamiji[a,1,*], Sunday Adewale Akintelu[b,1], David O Adekunle[a], David Gbenga Oke[a], Adesoji Alani Olanrewaju[a], Omowumi Temitayo Akinola[c]

[a] *Industrial Chemistry Programme, Bowen University, PMB 284, Iwo, Osun State, Nigeria*
[b] *Department of pure and Applied Chemistry, Ladoke Akintola University of Technology, PMB 4000, Ogbomoso, Oyo State, Nigeria*
[c] *Microbiology Programme, Bowen University, PMB 284 Iwo, Osun State, Nigeria*

A R T I C L E I N F O

Article history:
Received 14 February 2024
Revised 22 May 2024
Accepted 23 May 2024
Available online 29 May 2024

Dataset link: Insilico Evaluation on Potential Mt-Sp1/Matriptase Inhibitors Data: DFT and Molecular Modelling Approaches (Original data)

Keywords:
Mt-Sp1/Matriptase
Inhibitors
GFA
DFT
Docking
Target prediction

A B S T R A C T

Nine heterocyclic compounds were investigated using density functional theory, molecular operating environment software, material studio, swissparam (Swiss drug design) software. In this work, the descriptors generated from the optimized compounds proved to be efficient and explain the level of reactivity of the investigated compound. The developed quantitative structure activity relationship (QSAR) model was predictive and reliable. Also, compound 9 proved to be capable of inhibiting Mt-Sp1/Matriptase (pdb id: 1eax) than other examined heterocyclic compounds. Target prediction analysis was carried out on the compound with highest binding affinity (Compound 9) and the results were reported.

* Corresponding author.
E-mail address: abel.oyebamiji@bowen.edu.ng (A.K. Oyebamiji).
Social media: @OyebamijiAbel (A.K. Oyebamiji)
[1] The authors contributed equally.

https://doi.org/10.1016/j.dib.2024.110565

Specification Table

Subject	Computational Analysis
Specific subject area	Therapeutic and reactivity prediction
Type of data	QSAR Figure Table Mathematical model
How data were acquired	Spartan'14, Optimization, Material studio, PADEL, MOE, GFA
Data format	Raw Data and Predicted data
Description of data collection	Nine active compounds were optimized using B3LYP via 6-31G** as basis set. The density functional theory calculation was finalised at different time and this could be attributed to different atoms attached to the main compound under investigation. The calculated descriptors were subjected to material studio for QSAR analysis. The optimized compounds were docked against the repaired and prepared Mt-Sp1/Matriptase (receptor) and further subjected to other biological investigations.
Data source location	Computational Chemistry Research Laboratory, Industrial Chemistry Programme, BOWEN University, Iwo, Osun State, Nigeria
Data accessibility	The experimental and predicted data can be accessed in the data article (https://data.mendeley.com/datasets/y323rrk4h6/1); DOI: 10.17632/y323rrk4h6.1

1. Value of the Data

- The 2D structures of the compounds under investigation will help the scientists to know the exact atom and the types of bonds as well as the position of the derivatives involved in the molecules.
- The calculated features obtained from the optimized compounds (2D and 3D) will enable the researchers to fully understand the properties and the level of reactivity of the examined compounds.
- The predicted orbital energies will reveal the highest occupied molecular orbital and lowest unoccupied molecular orbital energies of the investigated molecules.
- The predicted QSAR model properties explained the suitable combination of descriptors with efficient predicting power.
- The observed binding sites in the observed target (PDB ID: 1eax) will explain to scientists the exact position that is best for binding of ligands.
- The calculated Fukui function will explain to researchers the appropriate point of attack in the reacting system.

2. Background

The objectives of this work are:

(i) To reveal the possible electrophilic and nucleophilic point of attack on the reacting species.
(ii) To identify the efficient quantitative structure activity relationship model for the purpose of analysing and predicting compounds.
(iii) To expose the level of reactivity of the compounds under investigation.

3. Data Description

Table 1 revealed the two dimensional structure of the ligand under investigation which was converted to 3D format for optimization purpose. Series of atoms (carbon, oxygen, nitrogen, sulphur, Chlorine, Bromine) were combined together to form the appropriate molecules under investigation.

Table 1
2D structure of the examined compounds.

S/N	2D Structures
1	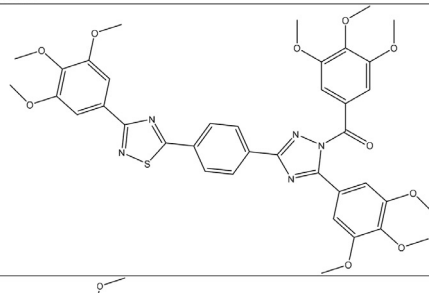
2	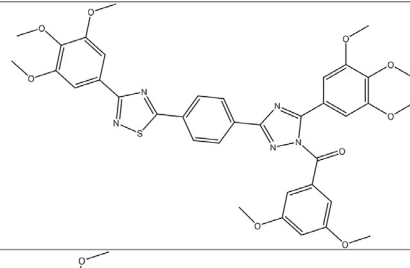
3	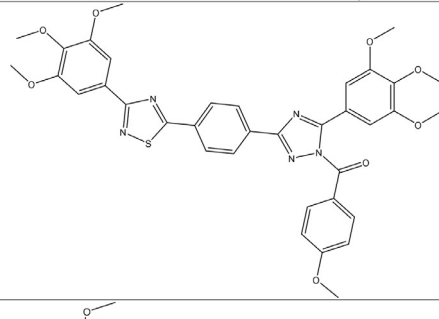
4	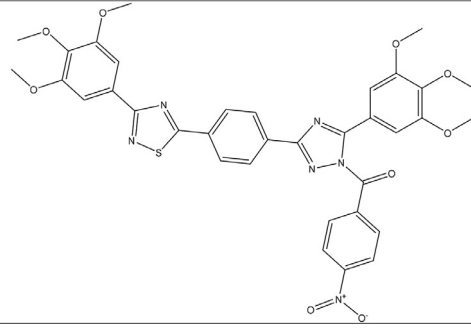

(*continued on next page*)

As shown in Table 2, series of properties were obtained from two and three dimensional structures of the investigated ligands. The properties obtained from two dimensional structures of the ligands were nC, nO, ATS4m, ATS5m, ATS6m, ATS7m, ATS8m, ATS0v, ATS2v and ATS3v (Figs. 2–9).

Table 1 (*continued*)

5	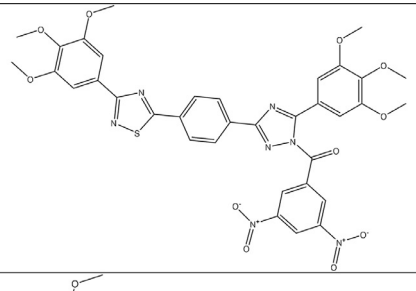
6	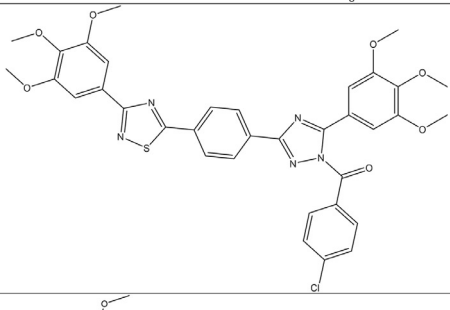
7	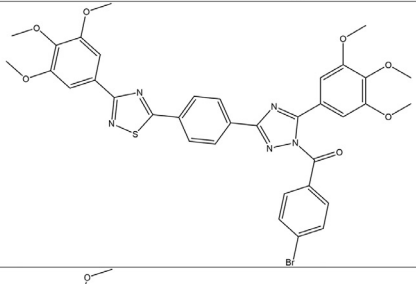
8	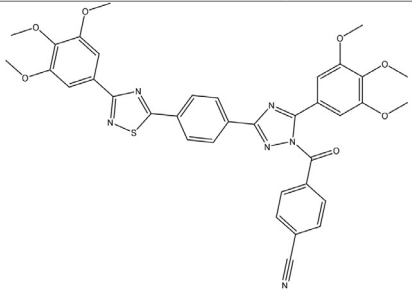
9	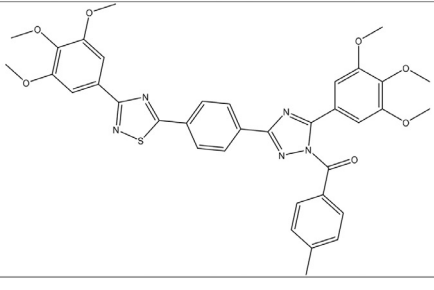

Table 2
Calculated descriptors for the 2D configuration of the examined compounds.

Name	nC	nO	ATS4m	ATS5m	ATS6m	ATS7m	ATS8m	ATS0v	ATS2v	ATS3v
1	35	10	18,049.25	16,949.23	16,680.48	16,589.33	15,690.71	19,763.94	34,835.84	40,248.77
2	36	9	17,334.63	16,770.38	16,936.87	16,973.14	15,737.76	20,033.24	35,348.01	39,895.44
3	33	8	15,583.07	14,430.65	14,623.79	14,545.64	13,530.34	18,359.79	32,558.25	36,743.7
4	32	9	16,002.91	14,608.34	14,761.67	15,057.22	13,883.87	18,302.73	32,653.85	36,809.84
5	32	11	17,473.44	17,243.38	17,672.35	16,412.6	15,927.49	18,947.74	33,888.25	38,545.07
6	32	7	15,470.53	14,417.06	15,020.76	14,654.99	13,866.8	18,130.61	32,113.97	35,957.28
7	32	7	16,094.09	14,951	16,354.65	15,811.59	15,557.34	18,330.04	32,281.6	36,170.32
8	33	7	15,506.46	14,332.01	14,485.69	14,465.45	13,339.87	18,293.47	32,358.03	36,501.5
9	33	7	15,220.49	14,177.95	14,353.77	14,135.89	13,054.12	18,143.4	32,474.48	36,547.9

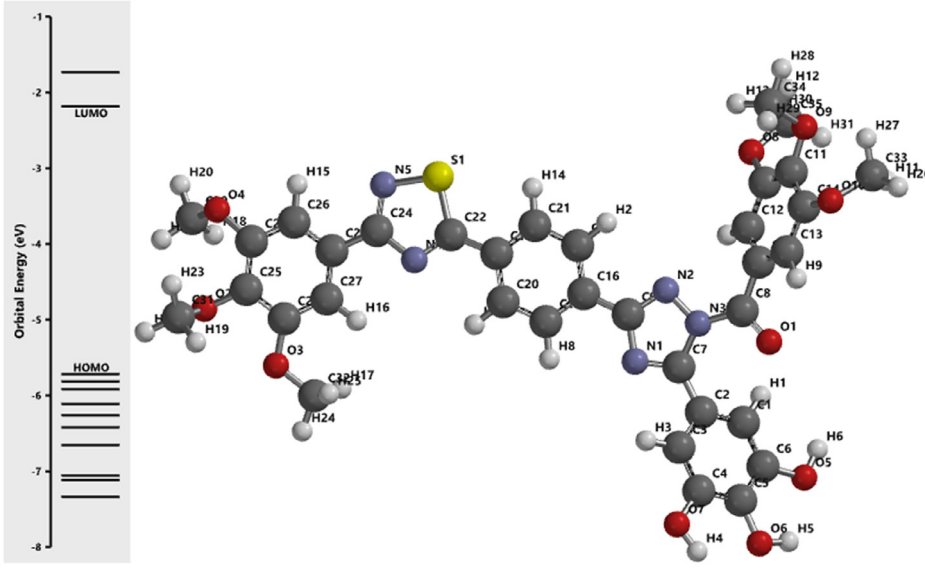

Fig. 1. Orbital energy for compound 1.

The spot that are rich in HOMO and LUMO on the investigated compounds were presented in Table 3. The HOMO-LUMO was graphically displayed in Figs. 1–10 and the graph ranges from −1 to −8 showing the orbital energy for each of the investigated compound.

Table 4 expose the analysis type and genetic function approximation of the developed QSAR model predicted from the observed% inhibition concentration and the calculated descriptors. The developed model was validated and the factors considered were Friedman LOF, R-squared, Adjusted R-squared and Cross validated R-squared, Significant Regression, Significance-of-regression F-value, Critical SOR F-value (95 %), Replicate points, Computed experimental error, Lack-of-fit points, Min expt. error for non-significant LOF (95 %) (Table 5). The predicted% inhibition concentration using the developed model shown in Table 4 were presented in Table 6.

Table 7 revealed the dimensions and the probable features of each of the active site predicted in Mt-Sp1/Matriptase (PDB ID: 1eax). The predicted size, propensity for ligand binding (PLB), hydrophobic regions, sides and residues were 62, 2.47, 9, 25, HIS57 PHE99 TYR146 ASP189 SER190 CYS191 GLN192 GLY193 ASP194 SER195 VAL213 SER214 TRP215 GLY216 ASP217 GLY219 CYS220 ALA221 GLY226 VAL227 TYR228 for site 1; 50, 2.05, 16, 24, ALA22 ASP23 GLU24 GLY25 GLU26 TRP27 PRO28 TRP29 GLN30 LEU68 GLY69 LEU70 HIS71 MET117 TRP141 LEU155 for site 2; 6, 1.19, 5, 11, LYS134 ALA135 ILE136 TRP137 GLU159 SER200 SER201 VAL202 for site 3; 36, 0.66, 17, 31, ILE41 CYS42 HIS57 CYS58 TYR59 ILE60 ASP60B TYR60G ASP96 PHE99 GLN192

Table 3
HOMO-LUMO orbital energies for the examined compounds.

	HOMO	LUMO
1	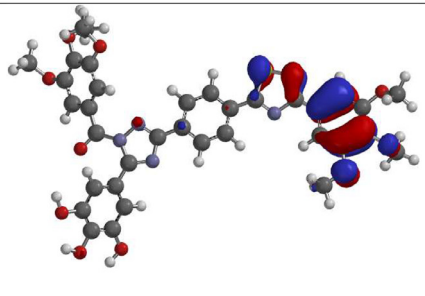	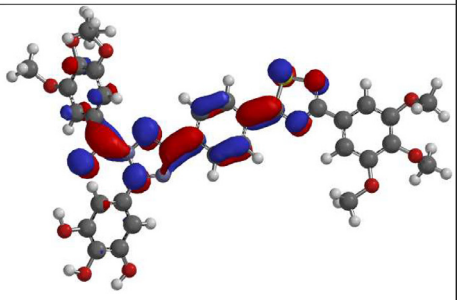
2	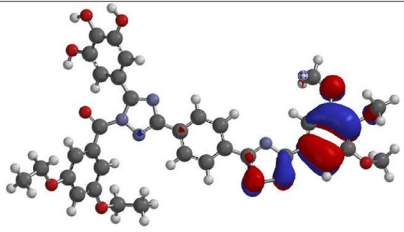	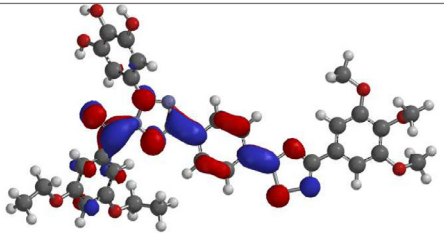
3	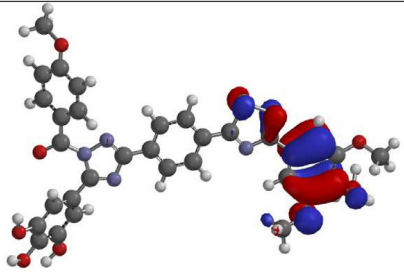	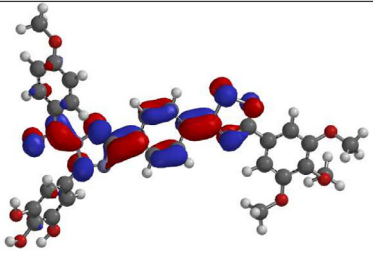
4	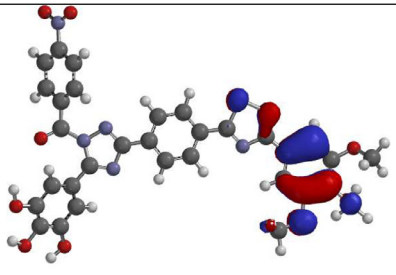	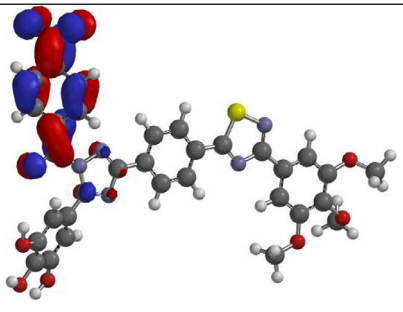

(*continued on next page*)

Table 3 (*continued*)

5	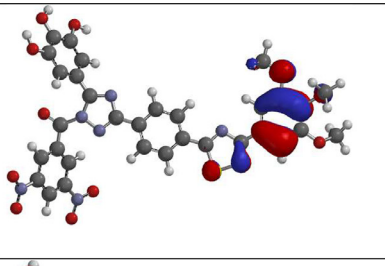	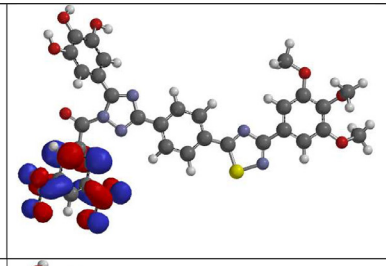
6	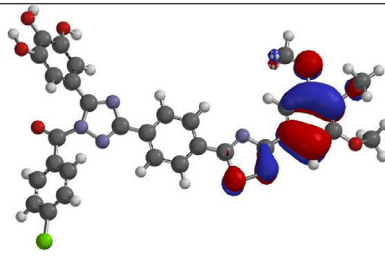	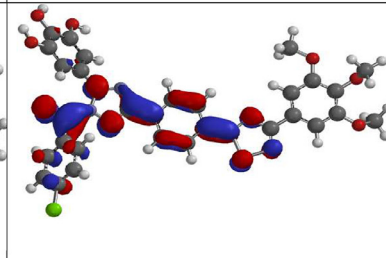
7	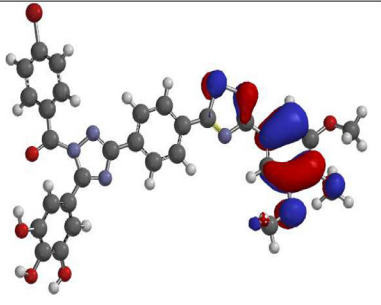	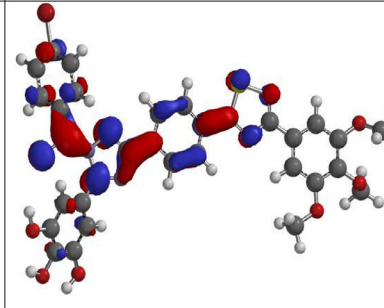
8	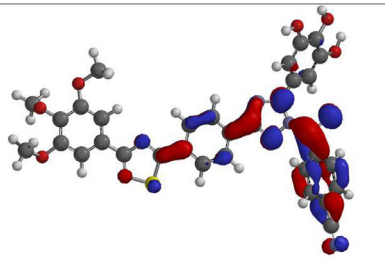	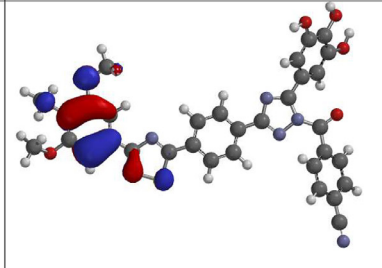
9	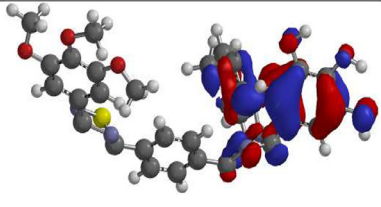	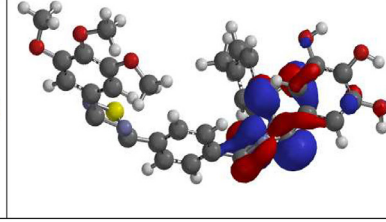

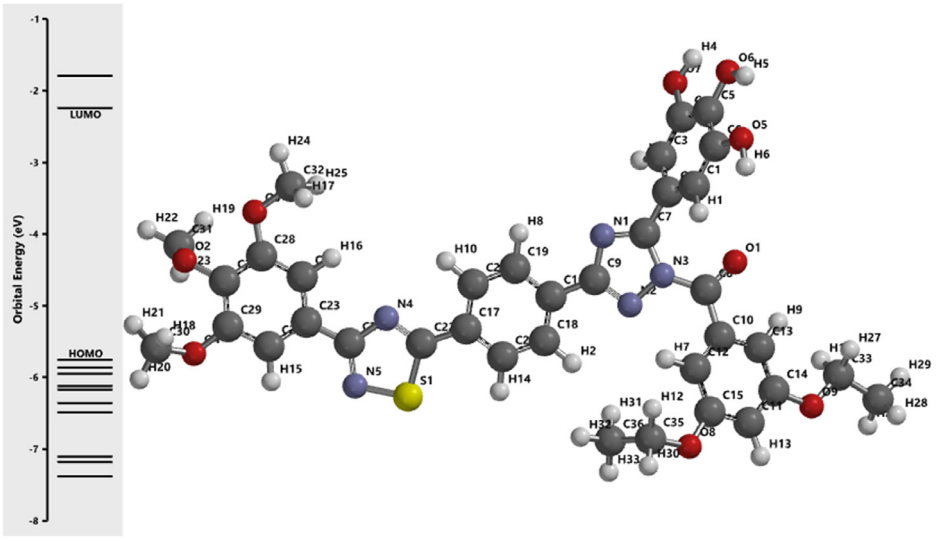

Fig. 2. Orbital energy for compound 2.

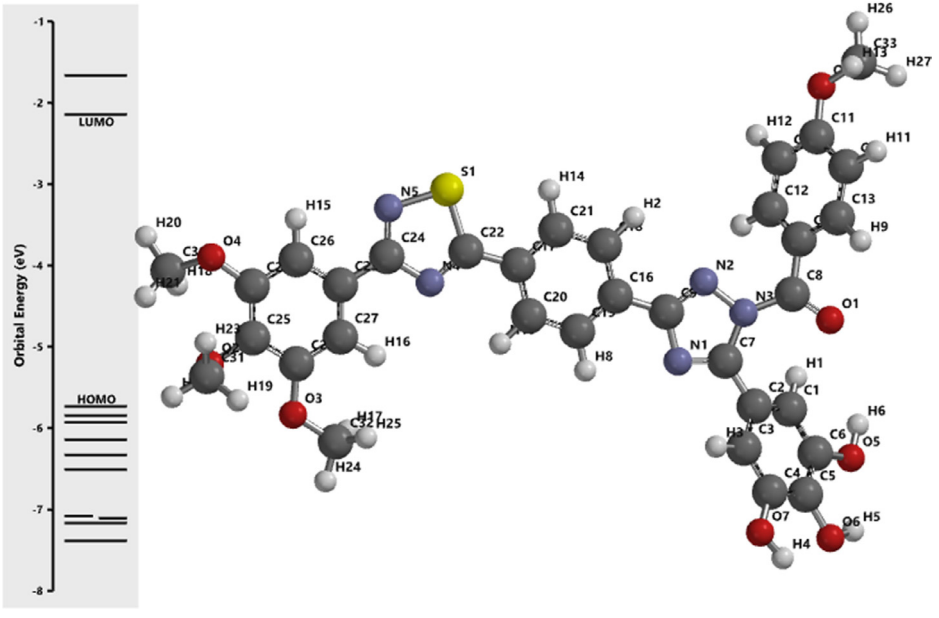

Fig. 3. Orbital energy for compound 3.

GLY193 SER195 for site 4; 36, 0.43, 17, 27, HIS128 VAL129 PHE130 PRO131 ALA132 VAL162 ILE163 ASN164 GLN165 MET181 ARG230 PRO232 LEU233 for site 5; 26, −0.07, 11, 26, THR65 VAL80 GLN81 GLU82 ARG83 ARG84 GLU109 LYS110 for site 6; 25, −0.17, 6, 14, HIS34 GLN38 GLY39 HIS40 GLN73 ARG76 TRP141 GLY151 ALA152 LEU153 for site 7; 5, −0.31, 4, 11, ALA56 TYR59 ILE60 ASP60A SER60H SER90 for site 8; 16, −0.44, 6, 13, ILE47 PRO120 ILE121 CYS122 LEU123 ASP125 ARG235 VAL244 for site 9; 13, −0.60, 11, 21, LEU123 PRO124 ASP125 HIS128 GLU203

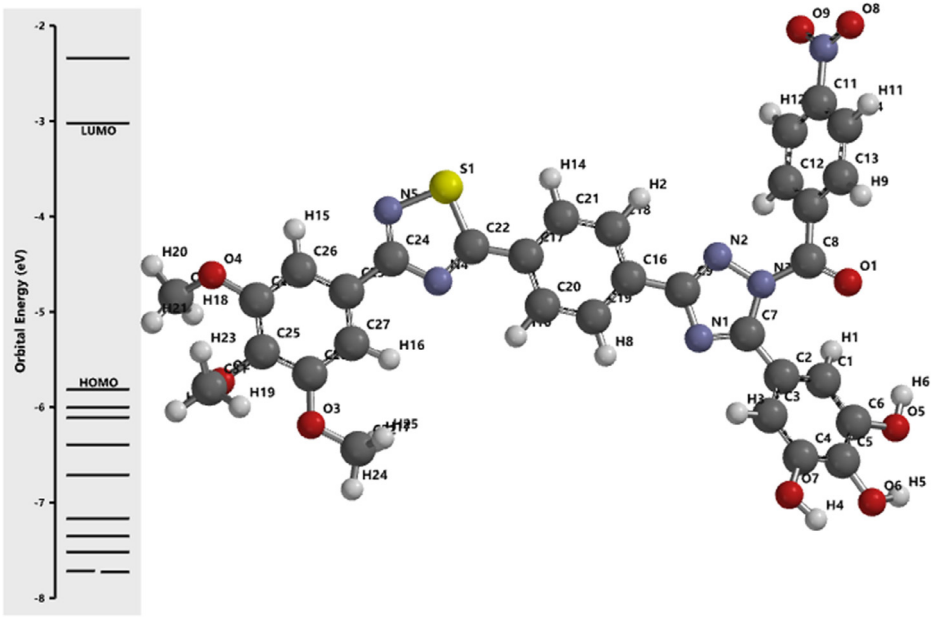

Fig. 4. Orbital energy for compound 4.

Table 4
Predicted model and the definition of the symbol from the optimized compounds.

Equation	Definition
Y = - 1.302298495 * X10	X10 : J : nO
- 0.022764411 * X14	X14 : N : ATS4m
+ 0.013434229 * X18	X18 : R : ATS8m
- 0.035004900 * X19	X19 : S : ATS0v
+ 0.021929774 * X22	X22 : V : ATS3v
+ 23.213368716	
Y = 7.677403070 * X8	X8 : H : nC
- 0.008772626 * X17	X17 : Q : ATS7m
+ 0.013873809 * X18	X18 : R : ATS8m
- 0.052359828 * X19	X19 : S : ATS0v
+ 0.019490443 * X21	X21 : U : ATS2v
+ 16.028600731	
Y = - 0.032796697 * X15	X15 : O : ATS5m
+ 0.034651247 * X16	X16 : P : ATS6m
- 0.013247239 * X18	X18 : R : ATS8m
- 0.022997371 * X19	X19 : S : ATS0v
+ 0.020042987 * X22	X22 : V : ATS3v
- 165.454606973	

PHE208 for site 10; 15, −0.64, 8, 13, TRP29 ARG119 PRO120 ILE121 CYS122 GLY205 ARG206 ILE207 for site 11; 8, −0.66, 3, 10, LEU36 PRO61 THR62 GLN63 TRP64 THR65 ARG84 LEU85 for site 12; 8, −0.67, 5, 7, ASP21 ALA152 LEU153 ILE154 GLN156 for site 13; 8, −0.72, 6, 19, HIS34 THR65 PHE67 ARG76 SER77 GLU82 for site 14; 5, −0.75, 5, 11, LEU172 GLN175 TRP215 ASP217 for site 15; 33, −0.79, 17, 24, PHE97 THR98 PHE99 GLN174 GLN175 MET180 TRP215, 4, −0.97, 1, 1, GLN174 GLN175 ILE176 THR177 for site 17.

Table 8 showed the calculated binding affinity, the amino acid residues (Figs. 10–19) and the type of interaction involved within the complex under investigation. The calculated binding affinity for compound 1–9 were −7.93345356 kcal/mol, −7.79621077 kcal/mol,

Table 5
Calculated features for the validation of the developed QSAR model.

	Equation 1	Equation 2	Equation 3
Friedman LOF	0.19719600	0.30365300	0.43646500
R-squared	0.99907500	0.99857600	0.99795300
Adjusted R-squared	0.99753400	0.99620200	0.99454100
Cross validated R-squared	0.97125600	0.95548800	0.95041100
Significant Regression	Yes	Yes	Yes
Significance-of-regression F-value	648.15479400	420.71009300	292.50930000
Critical SOR F-value (95 %)	9.61802100	9.61802100	9.61802100
Replicate points	0	0	0
Computed experimental error	0.00000000	0.00000000	0.00000000
Lack-of-fit points	3	3	3
Min expt. error for non-significant LOF (95 %)	0.10635400	0.13197600	0.15822700

Table 6
The actual and the predicted values from the developed model.

Actual values for W : ic50	Equation 1: predicted values	Equation 1: residual values	Equation 2: predicted values	Equation 2: residual values	Equation 3: predicted values	Equation 3: residual values
0.83000000	0.91406300	−0.08406300	1.02491800	−0.19491800	0.99420700	−0.16420700
1.98000000	1.94112800	0.03887200	1.87030400	0.10969600	1.84624700	0.13375300
2.76000000	2.92343300	−0.16343300	2.75588100	0.00411900	2.98733100	−0.22733100
0.19000000	0.26114300	−0.07114300	0.34653000	−0.15653000	−0.10821600	0.29821600
7.23000000	7.10995900	0.12004100	7.09536000	0.13464000	7.20324500	0.02675500
2.13000000	2.08465400	0.04534600	2.12827500	0.00172500	2.23981700	−0.10981700
8.22000000	8.29136800	−0.07136800	8.26058400	−0.04058400	8.23757300	−0.01757300
0.60000000	0.42132100	0.17867900	0.38732600	0.21267400	0.63088300	−0.03088300
9.37000000	9.36293100	0.00706900	9.44082200	−0.07082200	9.27891300	0.09108700

Table 7
Features of the predicted binding sites.

Site	Size	PLB	Hyd	Side	Residues
1	62	2.47	9	25	1:(HIS57 PHE99 TYR146 ASP189 SER190 CYS191 GLN192 GLY193 ASP194 SER195 VAL213 SER214 TRP215 GLY216 ASP217 GLY219 CYS220 ALA221 GLY226 VAL227 TYR228)
2	50	2.05	16	24	1:(ALA22 ASP23 GLU24 GLY25 GLU26 TRP27 PRO28 TRP29 GLN30 LEU68 GLY69 LEU70 HIS71 MET117 TRP141 LEU155)
3	6	1.19	5	11	1:(LYS134 ALA135 ILE136 TRP137 GLU159 SER200 SER201 VAL202)
4	36	0.66	17	31	1:(ILE41 CYS42 HIS57 CYS58 TYR59 ILE60 ASP60B TYR60G ASP96 PHE99 GLN192 GLY193 SER195)
5	36	0.43	17	27	1:(HIS128 VAL129 PHE130 PRO131 ALA132 VAL162 ILE163 ASN164 GLN165 MET181 ARG230 PRO232 LEU233)
6	26	−0.07	11	26	1:(THR65 VAL80 GLN81 GLU82 ARG83 ARG84 GLU109 LYS110)
7	25	−0.17	6	14	1:(HIS34 GLN38 GLY39 HIS40 GLN73 ARG76 TRP141 GLY151 ALA152 LEU153)
8	5	−0.31	4	11	1:(ALA56 TYR59 ILE60 ASP60A SER60H SER90)
9	16	−0.44	6	13	1:(ILE47 PRO120 ILE121 CYS122 LEU123 ASP125 ARG235 VAL244)
10	13	−0.60	11	21	1:(LEU123 PRO124 ASP125 HIS128 GLU203 PHE208)
11	15	−0.64	8	13	1:(TRP29 ARG119 PRO120 ILE121 CYS122 GLY205 ARG206 ILE207)
12	8	−0.66	3	10	1:(LEU36 PRO61 THR62 GLN63 TRP64 THR65 ARG84 LEU85)
13	8	−0.67	5	7	1:(ASP21 ALA152 LEU153 ILE154 GLN156)
14	8	−0.72	6	19	1:(HIS34 THR65 PHE67 ARG76 SER77 GLU82)
15	5	−0.75	5	11	1:(LEU172 GLN175 TRP215 ASP217)
16	33	−0.79	17	24	1:(PHE97 THR98 PHE99 GLN174 GLN175 MET180 TRP215)
17	4	−0.97	1	1	1:(GLN174 GLN175 ILE176 THR177)

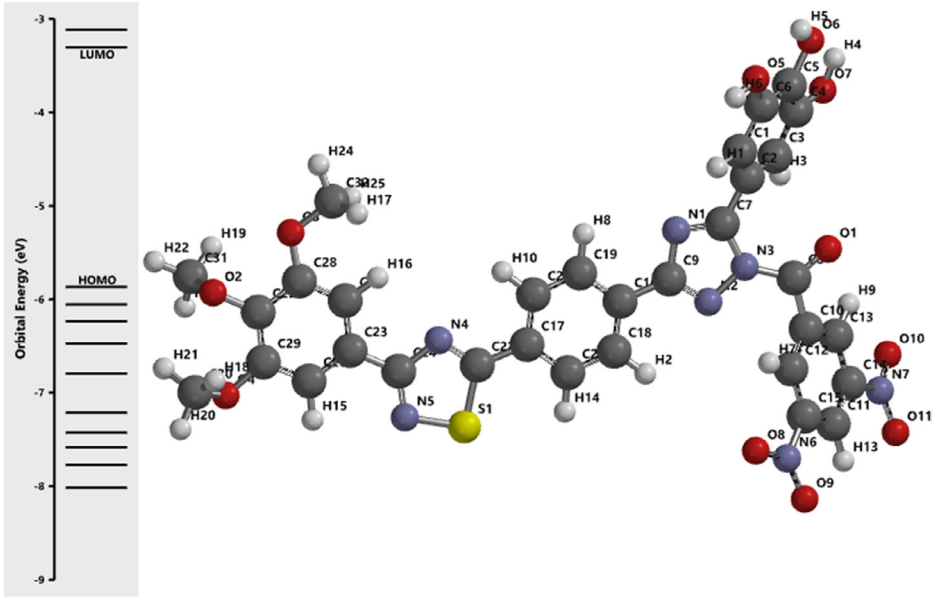

Fig. 5. Orbital energy for compound 5.

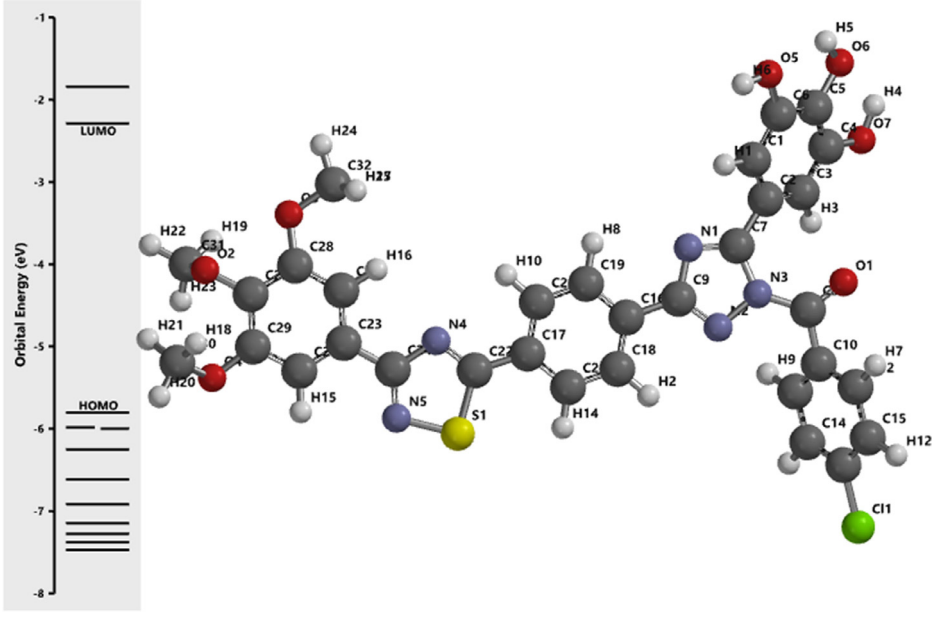

Fig. 6. Orbital energy for compound 6.

−7.98120165 kcal/mol, −8.48985958 kcal/mol, −8.28229141 kcal/mol, −8.13518143 kcal/mol, −7.86430264 kcal/mol, −8.09322929 kcal/mol and −8.80468273 kcal/mol respectively. Also, the electrophilic and nucleophhilic point of attack by electrophile and nucleophile were reported in Table 9.

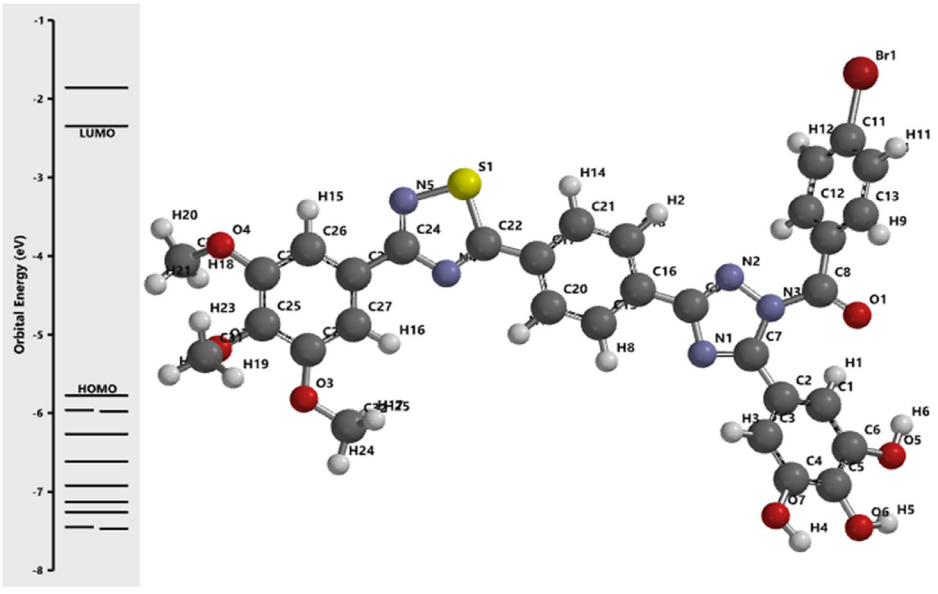

Fig. 7. Orbital energy for compound 7.

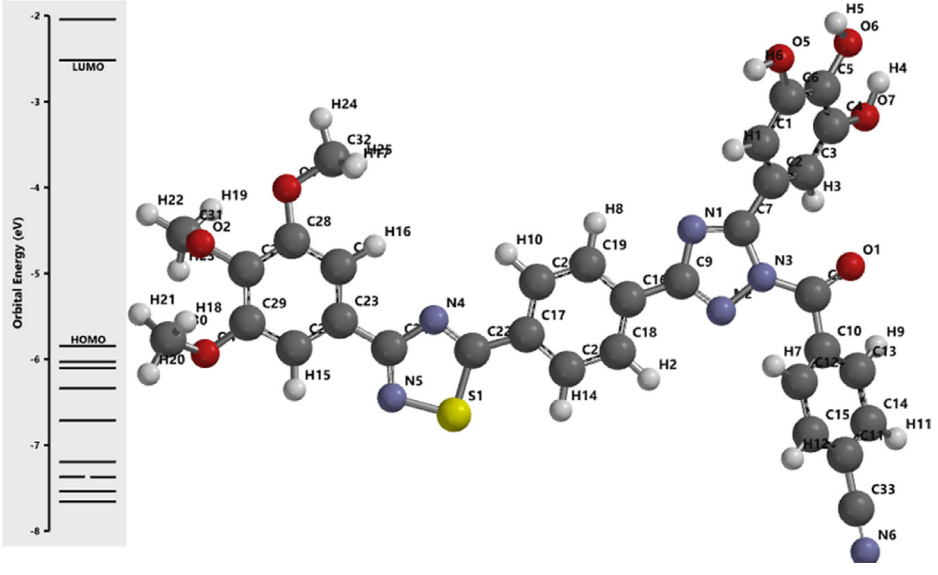

Fig. 8. Orbital energy for compound 8.

4. Experimental Design, Materials, and Methods

The heterocyclic compounds [1] under investigation were sketched using Chemoffice software [2] before converted to 3D format for optimization purpose using Spartan 14 software [3]. Series of properties were obtained from the optimized structure and were reported accordingly. The obtained properties were subjected to material studio software [4] for QSAR development which

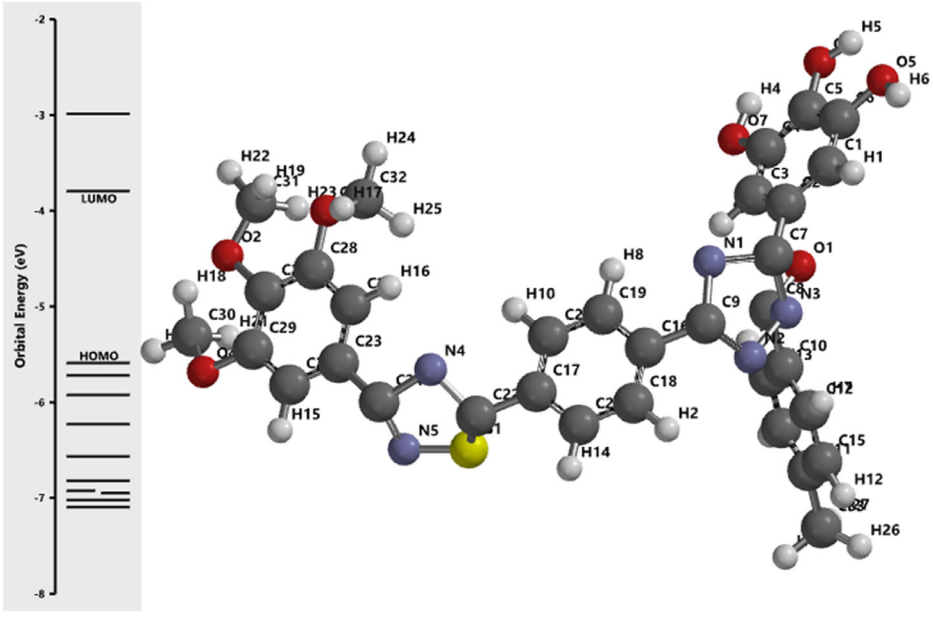

Fig. 9. Orbital energy for compound 9.

Table 8
Calculated scoring and the predicted interactions.

	Binding Affinity (kcal/mol)	Ligand	Receptor		Interaction	Distance	E (kcal/mol)
1	−7.93345356	5-ring	CA	ILE 41(A)	pi-H	4.16	−0.6
		6-ring	CE1	HIS143(A)	pi-H	4.24	−0.5
2	−7.79621077	5-ring	CG1	VAL 244(A)	pi-H	4.01	−1.1
3	−7.98120165	O43 64	OG	SER 60(A)	H-donor	2.98	−0.6
		6-ring	ND2	ASN 241(A)	pi-H	3.63	−0.7
4	−8.48985958	O 68	SG	CYS 42 (A)	H-donor	3.44	−2.0
		O 71	OD2	ASP 60 (A)	H-donor	3.24	−1.7
		O 73	O	ILE 60 (A)	H-donor	3.35	−1.6
		O 68	NE2	HIS 57 (A)	H-acceptor	3.15	−1.3
		5-ring	CB	HIS 40 (A)	pi-H	3.98	−1.0
5	−8.28229141	O 65	O	ILE 60 (A)	H-donor	3.38	−0.7
		O 67	OD2	ASP 60 (A)	H-donor	3.36	−1.1
		O 77	OD1	ASP 60 (A)	H-donor	3.23	−2.5
		6-ring	6-ring	TYR 60 (A)	pi-pi	3.98	−0.0
6	−8.13518143	O 68	O	HIS 57 (A)	H-donor	2.97	−2.7
		6-ring	CB	HIS 40 (A)	pi-H	4.18	−0.9
		6-ring	CG2	ILE 41 (A)	pi-H	4.26	−0.7
7	−7.86430264	O 64	O	LEU 85 (A)	H-donor	2.92	−0.8
8	−8.09322929	O 66	O	ILE 60 (A)	H-donor	3.26	−0.5
		O 68	OD2	ASP 60 (A)	H-donor	3.06	−2.3
		6-ring	CA	ILE 41 (A)	pi-H	4.44	−0.9
		6-ring	NE2	GLN 192 (A)	pi-H	4.10	−1.4
9	−8.80468273	6-ring	CG2	ILE 41(A)	pi-H	4.12	−0.8
		6-ring	NE2	GLN 192(A)	pi-H	4.03	−0.6
Ref	−7.14661407	O42 73	N	GLY 193 (A)	H-acceptor	3.28	−1.2

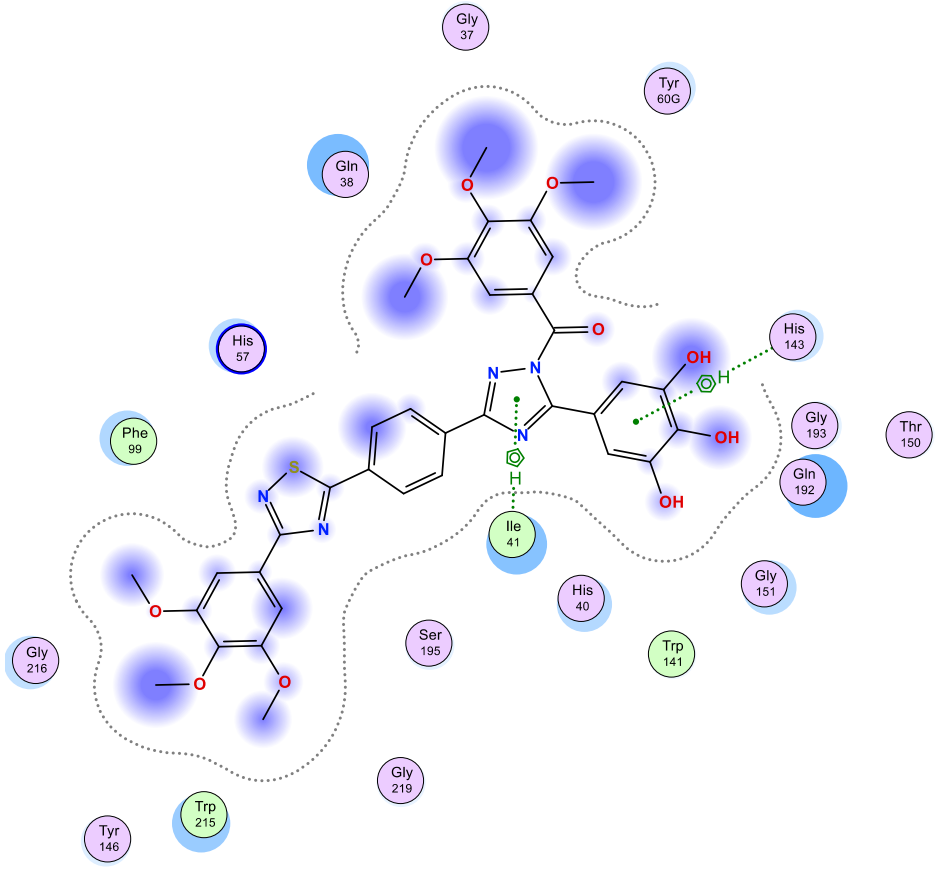

Fig. 10. Compound 1 in the binding site of Mt-Sp1/Matriptase surrounded with amino acid residues.

therefore generated various data such as type and genetic function approximation, the developed model together with the symbol in the individual model, features for the validation and actual and the predicted values from the developed model. The inhibiting activities of the optimized compounds were accomplished using docking via molecular operating environments software [5–12] and the scoring for each docked complex was obtained and reported.

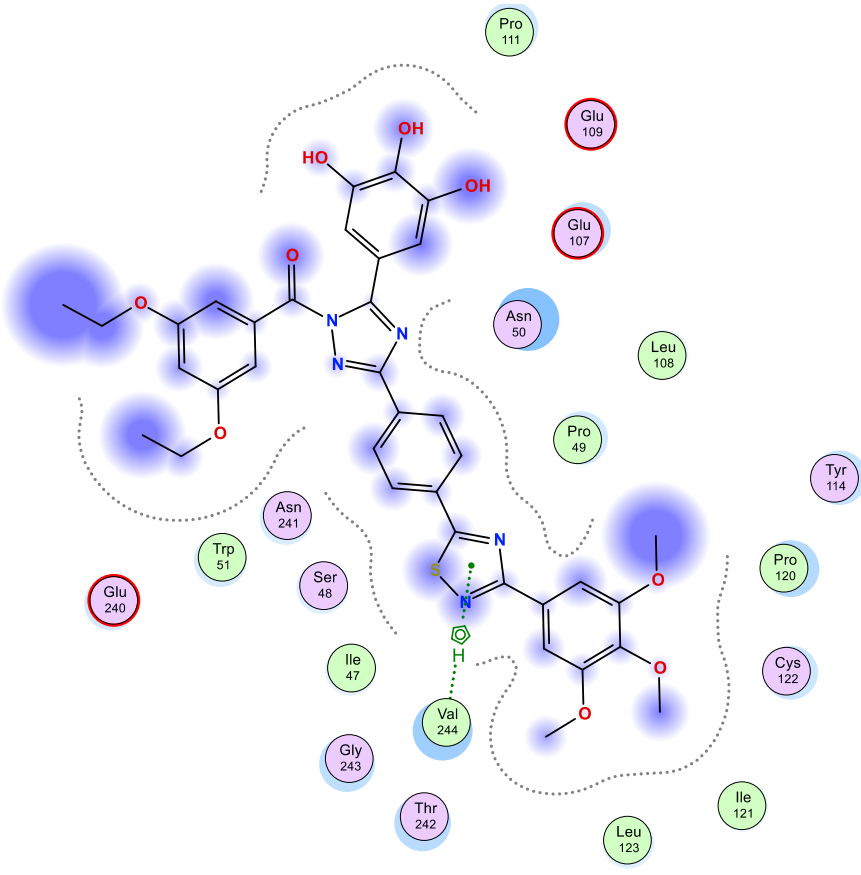

Fig. 11. Compound 2 in the binding site of Mt-Sp1/Matriptase surrounded with amino acid residues.

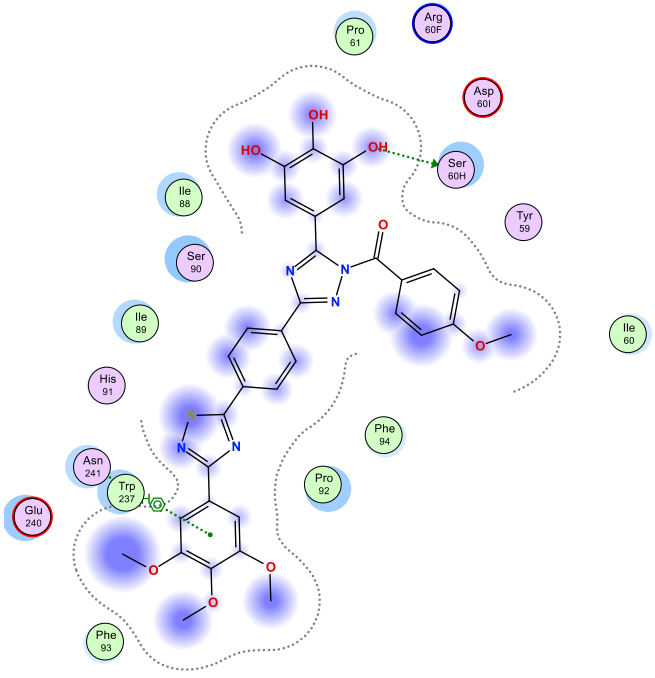

Fig. 12. Compound 3 in the binding site of Mt-Sp1/Matriptase surrounded with amino acid residues.

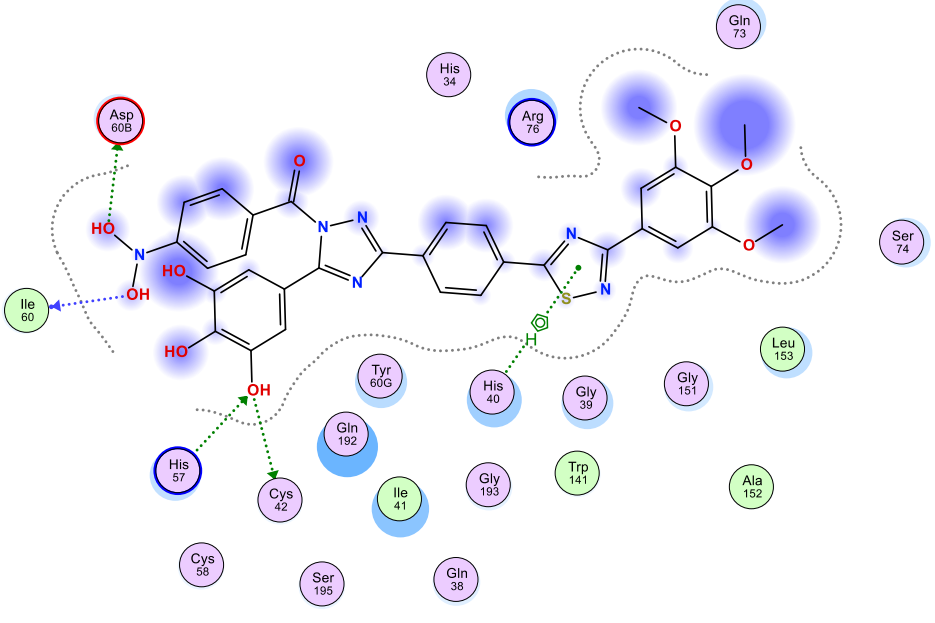

Fig. 13. Compound 4 in the binding site of Mt-Sp1/Matriptase surrounded with amino acid residues.

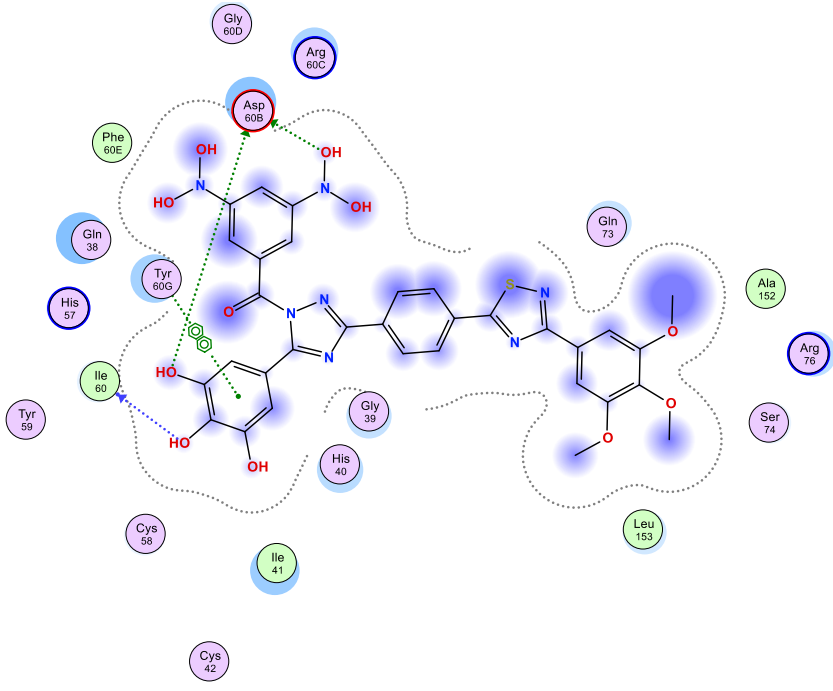

Fig. 14. Compound 5 in the binding site of Mt-Sp1/Matriptase surrounded with amino acid residues.

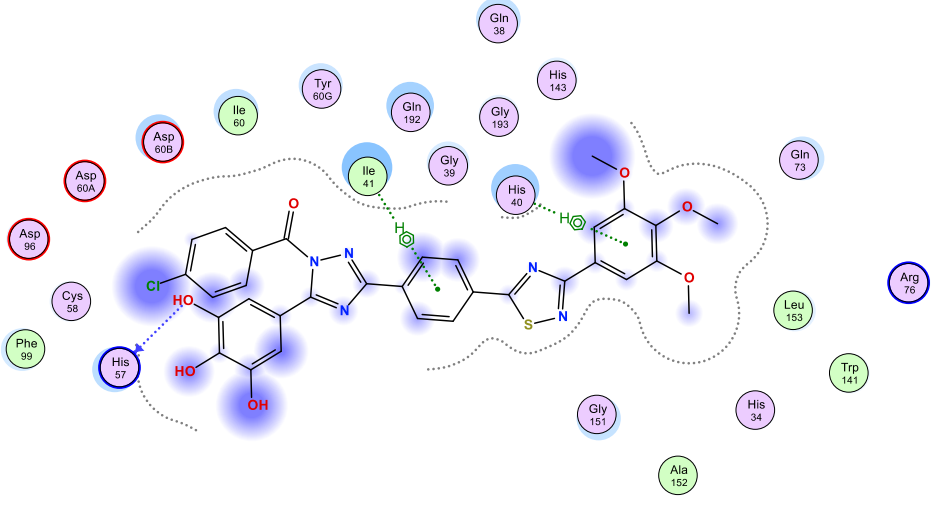

Fig. 15. Compound 6 in the binding site of Mt-Sp1/Matriptase surrounded with amino acid residues.

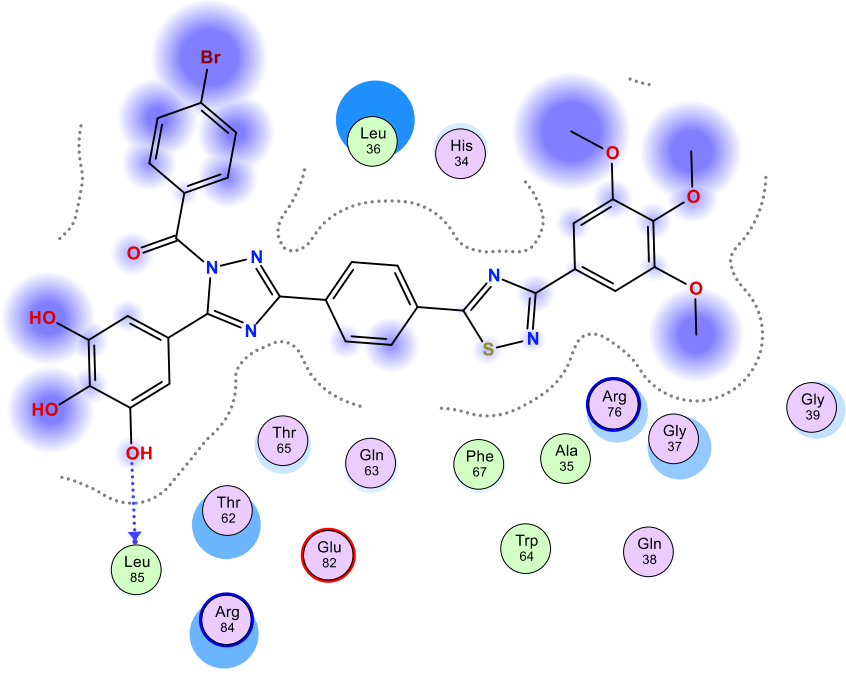

Fig. 16. Compound 7 in the binding site of Mt-Sp1/Matriptase surrounded with amino acid residues.

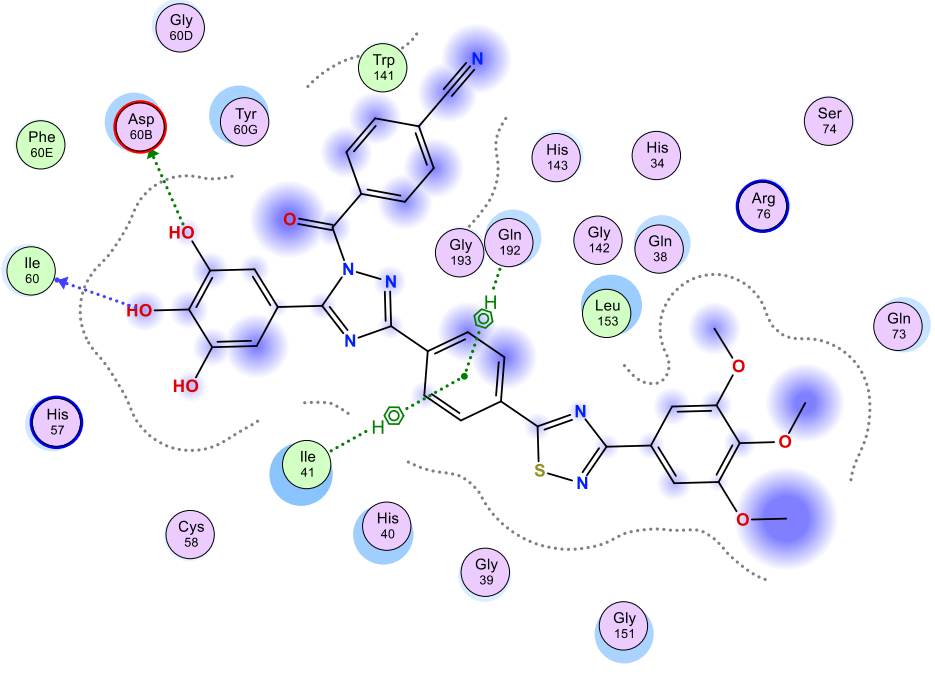

Fig. 17. Compound 8 in the binding site of Mt-Sp1/Matriptase surrounded with amino acid residues.

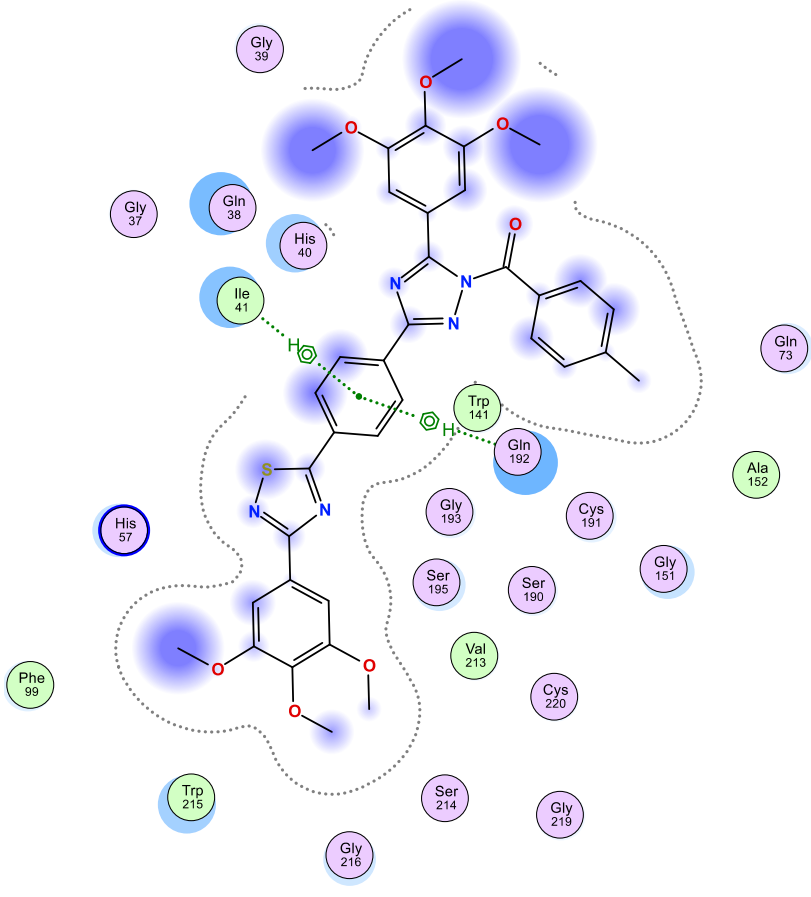

Fig. 18. Compound 9 in the binding site of Mt-Sp1/Matriptase surrounded with amino acid residues.

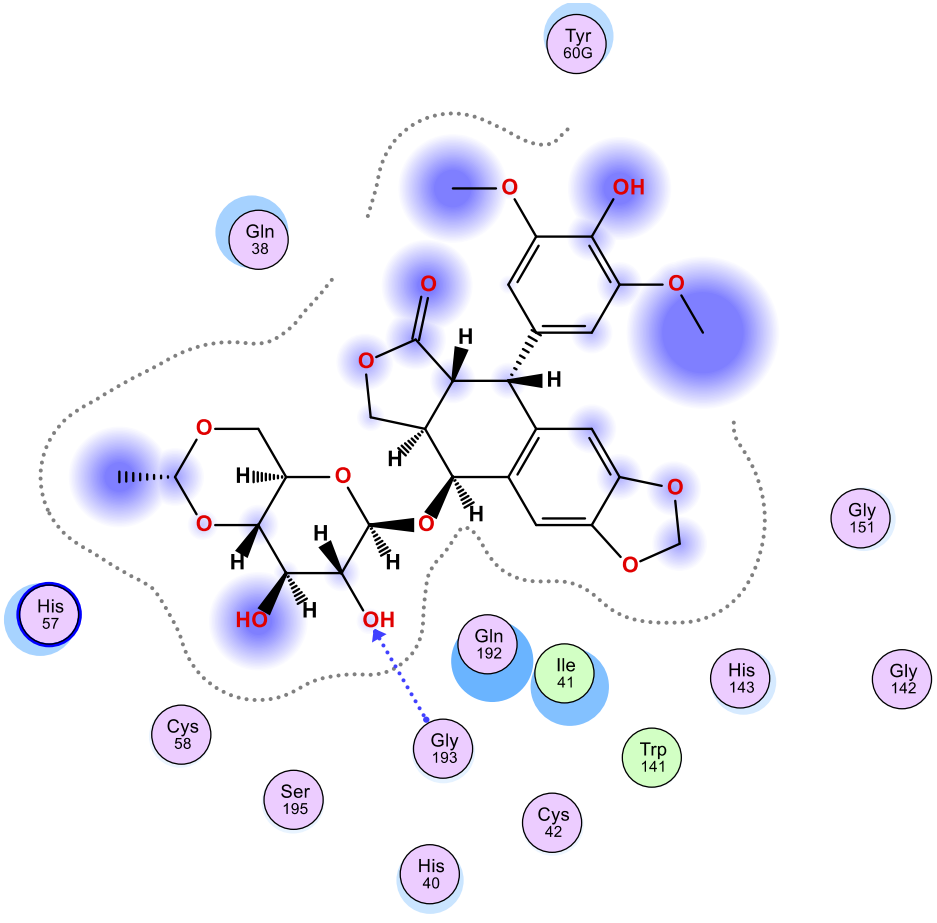

Fig. 19. Reference compound (Etoposide) in the binding site of Mt-Sp1/Matriptase surrounded with amino acid residues.

Table 9
Fukui function indices for compound **9**.

Atom	$P_{N(r)}$	$P_{N+1(r)}$	$P_{N-1(r)}$	f^+	f^-
C10	0.065	0.062	0.055	−0.003	0.010
C8	0.516	0.391	0.432	−0.125	0.084
O1	−0.461	−0.497	−0.386	−0.036	−0.075
N3	−0.391	−0.317	−0.293	0.074	−0.098
N2	−0.363	−0.321	−0.223	0.042	−0.140
C7	0.435	0.135	0.209	−0.300	0.226
C9	0.409	0.166	0.249	−0.243	0.160
N1	−0.527	−0.447	−0.352	0.080	−0.175
C1	−0.116	−0.174	−0.145	−0.058	0.029
C2	0.075	0.140	0.129	0.065	−0.054
C3	−0.123	−0.072	−0.077	0.051	−0.046
C4	0.316	0.302	0.337	−0.014	−0.021
C5	0.270	0.251	0.291	−0.019	−0.021
C6	0.298	0.276	0.321	−0.022	−0.023
O5	−0.600	−0.620	−0.559	−0.02	−0.041
O6	−0.597	−0.622	−0.574	−0.025	−0.023
O7	−0.569	−0.593	−0.550	−0.024	−0.019
C16	0.098	0.098	0.081	0.000	0.017
C18	−0.126	−0.100	−0.091	0.026	−0.035
C21	−0.147	−0.113	−0.103	0.034	−0.044
C17	0.118	0.020	0.024	−0.098	0.094
C20	−0.108	−0.097	−0.083	0.011	−0.025
C19	−0.121	−0.104	−0.102	0.017	−0.019
C22	0.044	−0.055	−0.037	−0.099	0.081
S1	0.385	0.547	0.601	0.162	−0.216
N4	−0.490	−0.424	−0.413	0.066	−0.077
C24	0.379	0.163	0.200	−0.216	0.179
N5	−0.537	−0.477	−0.443	0.060	−0.094
C23	0.084	0.065	0.066	−0.019	0.018
C26	−0.171	−0.136	−0.119	0.035	−0.052
C29	0.321	0.277	0.297	−0.044	0.024
C27	−0.187	−0.166	−0.154	0.021	−0.033
C28	0.342	0.316	0.330	−0.026	0.012
C25	0.251	0.313	0.342	0.062	−0.091
O4	−0.532	−0.529	−0.500	0.003	−0.032
O3	−0.527	−0.548	−0.528	−0.021	0.001
C32	−0.078	−0.097	−0.107	−0.019	0.029
O2	−0.525	−0.544	−0.502	−0.019	−0.023
C31	−0.078	−0.068	−0.089	0.010	0.011
C30	−0.070	−0.121	−0.144	−0.051	0.074

Limitations

Optimization of compounds for quantum chemical analysis requires basis set. For further investigation, higher basis set is advisable so as to obtained more detailed descriptors.

Acknowledgement

We are grateful to the computational chemistry research laboratory, Industrial Chemistry Programme, BOWEN University, Nigeria for the computational resources and Mrs E.T. Oyebamiji and Miss Priscilla F. Oyebamiji for their assistance in the course of this work.

Ethics Statement

This study does not involve studies with animals and humans.

Data Availability

Insilico Evaluation on Potential Mt-Sp1/Matriptase Inhibitors Data: DFT and Molecular Modelling Approaches (Original data) (Mendeley Data)

CRediT Author Statement

Abel Kolawole Oyebamiji: Conceptualization, Methodology, Data curation, Writing – original draft, Visualization, Investigation, Writing – review & editing; **Sunday Adewale Akintelu:** Conceptualization, Methodology, Data curation, Writing – original draft, Visualization, Investigation, Writing – review & editing; **David O Adekunle:** Methodology, Data curation, Writing – review & editing; **David Gbenga Oke:** Data curation, Visualization, Investigation; **Adesoji Alani Olanrewaju:** Methodology, Data curation, Writing – original draft; **Omowumi Temitayo Akinola:** Data curation, Writing – review & editing.

Declaration of Competing Interest

The authors declare that they have no known competing financial interests or personal relationships which have or could be perceived to have influenced the work reported in this article.

References

[1] Y.J. Pragathi, R. Sreenivasulu, D. Veronica, R. Raju, Design, synthesis, and biological evaluation of 1,2,4-thiadiazole-1,2,4-triazole derivatives bearing amide functionality as anticancer agents, Arab. J. Sci. Eng. 46 (2021) 225–232, doi:10.1007/s13369-020-04626-z.

[2] A.O. Ibrahim, B. Semire, T.E. Oladuji, D.F. Latona, A.K. Oyebamiji, A.D. Owonikoko, I.O. Abdulsalami, M.D. Adeoye, O.A. Odunola, Molecular properties and In silico bioactivity evaluation of (4-fluorophenyl)[5)-3-phen-(4-nitrophenyl yl-4,5-dihydro-1H-pyrazol-1-yl]methanone derivatives: DFT and molecular docking approaches, J. Taibah Univ. Med. Sci. 18 (6) (2023) 1386–1405.

[3] Y. Chinthala, S. Thakur, S. Tirunagari, S. Chinde, A.K. Domatti, N.K. Arigari, K. V N S S, S. Alam, K.K. Jonnala, F. Khan, A. Tiwari, P. Grover, Synthesis, docking and ADMET studies of novel chalcone triazoles for anti-cancer and anti-diabetic activity, Eur. J. Med. Chem. 93 (2015) 564–573.

[4] S.E. Adeniji, S. Uba, A. Uzairu, QSAR modeling and molecular docking analysis of some active compounds against*Mycobacterium tuberculosis* receptor (Mtb CYP121), J. Pathog. 24 (2018) 1018694, doi:10.1155/2018/1018694.

[5] P. Gopinath, M.K. Kathiravan, Docking studies and molecular dynamics simulation of triazole benzene sulfonamide derivatives with human carbonic anhydrase IX inhibition activity, RSC Adv. 11 (60) (2021) 38079–38093, doi:10.1039/d1ra07377j.

[6] P. Patel, R. Shakya, V.A. Vishakha, B.D. Kurmi, S.K. Verma, G.D. Gupta, H. Rajak, Furan and benzofuran derivatives as privileged scaffolds as anticancer agents: SAR and docking studies (2010 to till date), J. Mol. Struct. 1299 (2024) 137098.

[7] V. Asati, P. Ghode, S. Bajaj, S.K. Jain, S.K. Bharti, 3D-QSAR and molecular docking studies on oxadiazole substituted benzimidazole derivatives: validation of experimental inhibitory potencies towards COX-2, Curr. Comput. Aided Drug Des. 15 (4) (2019) 277–293, doi:10.2174/1573409914666181003153249.

[8] V. Asati, S.S. Thakur, N. Upmanyu, S.K. Bharti, Virtual screening, molecular docking, and DFT studies of some thiazolidine-2,4-diones as potential PIM-1 kinase inhibitors, Chemistryselect 3 (1) (2018) 127–135.

[9] A. Ali, A. Ali, V. Asati, S. Kaya, M.J. Ahsan, Design, synthesis and anti-hyperglycemic assessments of novel 5-benzylidenethiazolidine-2, 4-dione derivatives as PPAR-γ agonist, J. Indian Chem. Soc. 100 (11) (2023) 101100.

[10] R. S.P, G.D. Gupta, V. Asati, Design, synthesis and antidiabetic study of triazole clubbed indole derivatives as α-glucosidase inhibitors, Bioorg. Chem. 139 (2023) 106750, doi:10.1016/j.bioorg.2023.106750.

[11] S. Gupta, G.S. Baweja, G.D. Gupta, V. Asati, Identification of potential N-substituted 5-benzylidenethiazolidine-2,4dione derivatives as α-amylase inhibitors: computational cum synthetic studies, J. Mol. Struct. 1287 (2023) 135596.

[12] A. Anant, A. Ali, A. Ali, G.D. Gupta, V. Asati, A Computational approach to discover potential quinazoline derivatives against CDK4/6 kinase, J. Mol. Struct. 1245 (2021) 131079.